Brain Struct Funct
DOI 10.1007/s00429-008-0178-0

ORIGINAL ARTICLE

Norepinephrinergic afferents and cytology of the macaque monkey midline, mediodorsal, and intralaminar thalamic nuclei

Brent A. Vogt · Patrick R. Hof · David P. Friedman · Robert W. Sikes · Leslie J. Vogt

Received: 6 August 2007 / Accepted: 8 February 2008
© Springer-Verlag 2008

Abstract The midline and intralaminar thalamic nuclei (MITN), locus coeruleus (LC) and cingulate cortex contain nociceptive neurons. The MITN that project to cingulate cortex have a prominent innervation by norepinephrinergic axons primarily originating from the LC. The hypothesis explored in this study is that MITN neurons that project to cingulate cortex receive a disproportionately high LC input that may modulate nociceptive afferent flow into the forebrain. Ten cynomolgus monkeys were evaluated for dopamine-β hydroxylase (DBH) immunohistochemistry, and nuclei with moderate or high DBH activity were analyzed for intermediate neurofilament proteins, calbindin (CB), and calretinin (CR). Sections of all but DBH were thionin counterstained to assure precise localization in the mediodorsal and MITN, and cytoarchitecture was analyzed with neuron-specific nuclear binding protein. Moderate–high levels of DBH-immunoreactive (ir) axons were generally associated with high densities of CB-ir and CR-ir neurons and low levels of neurofilament proteins. The paraventricular, superior centrolateral, limitans and central nuclei had relatively high and evenly distributed DBH, the magnocellular mediodorsal and paracentral nuclei had moderate DBH-ir, and other nuclei had an even and low level of activity. Some nuclei also have heterogeneities in DBH-ir that raised questions of functional segregation. The anterior multiformis part of the mediodorsal nucleus but not middle and caudal levels had high DBH activity. The posterior parafascicular nucleus (Pf) was heterogeneous with the lateral part having little DBH activity, while its medial division had most DBH-ir axons and its multiformis part had only a small number. These findings suggest that the LC may regulate nociceptive processing in the thalamus. The well established role of cingulate cortex in premotor functions and the projections of Pf and other MITN to the limbic striatum suggests a specific role in mediating motor outflow for the LC-innervated nuclei of the MITN.

Keywords Dopamine-β hydroxylase · Cingulate cortex · Thalamus · Locus coeruleus · Stress · Pain

Abbreviations

ACC	Anterior cingulate cortex
AD	Anterodorsal nucleus
AV	Anteroventral nucleus
C	Central nucleus of the thalamus
Cif	Inferior part
Cl	Lateral part
Cim	Inferior medial part
Cs	Superior part
Csl	Superior lateral part
CB	Calbindin
cgs	Cingulate sulcus

B. A. Vogt (✉) · L. J. Vogt
Cingulum NeuroSciences Institute and SUNY Upstate Medical University, 4435 Stephanie Drive, Manlius, NY, USA
e-mail: bvogt@twcny.rr.com

P. R. Hof
Department of Neuroscience, Mount Sinai School of Medicine, New York, NY, USA

D. P. Friedman
Department of Physiology and Pharmacology, Wake Forest University School of Medicine, Winston-Salem, NC, USA

R. W. Sikes
Department of Physical Therapy, Northeastern University, Boston, MA, USA

CnMd (CM)	Centre medianum
CR	Calretinin
DBH	Dopamine-β hydroxylase
dPCC	Dorsal posterior cingulate cortex
Hb	Habenula
hit	Habenulointerpeduncular tract
ir	Immunoreactive
LD	Laterodorsal nucleus
Li	Limitans
MCC	Midcingulate cortex
MD	Mediodorsal nucleus and its divisions
MDdc	Densocellular
MDmc	Magnocellular
MDmf	Multiformis
MDmfa	Anterior multiformis part of MDmf
MDpc	Parvocellularis
mtt	Mammilothalamic tract
NeuN	Neuron-specific nuclear binding protein
PCC	Posterior cingulate cortex
Pcn	Paracentral nucleus of the thalamus
Pf	Parafascicular nucleus
Pfl	Lateral part
Pfm	Medial part
Pfmf	Multiformis part
PGi	Paragigantocellular nucleus of the reticular formation
Prt	Pretectal nucleus
Pt	Parataenial nucleus
Pulm	Medial pulvinar nucleus
Pv	Paraventricular nucleus
Re	Reuniens
sc	Superior colliculus
sm	Stria medullaris
SMI32	Antibody for nonphosphorylated intermediate neurofilaments
sPf	Subparafascicular nucleus
VM	Ventral medial (VLm of Olszewski)

Introduction

Almost every structure in the brain receives some input from the locus coeruleus (LC) and this led Foote (1997) to conclude that there is no readily evident organizational scheme for this vast efferent arbor with the basal ganglia being the only region not innervated. This widespread innervation led to the view of general functions for the LC, such as improving signal-to-noise ratios in sensory systems (Morrison and Foote 1986; Ebert 1996; Ego-Stengel et al. 2002; Devilbis and Waterhouse 2004), rather than roles in specific functions. Beyond this "widespread" perspective, however, there is the view that emphasizes targets with heaviest LC innervation and considers the consequences of heavy inputs in a system that is involved in flight-or-fight coordination (Abercrombie and Jacobs 1987). One example is the heavy projection of LC to the magnocellular division of the paraventricular nucleus of the hypothalamus that regulates vasopressin release (Ginsberg et al. 1994). The thalamus also has nuclei with particularly heavy LC/norepinephrinergic (NEergic) inputs including the midline and intralaminar thalamic nuclei (MITN) (Jones and Yang 1985). The LC, MITN, and their projections to cingulate cortex are involved in pain processing and fight-or-flight responses, yet the system organization and regulation by NE have not been explored.

Dopaminae-β hydroxylase (DBH) is the rate limiting enzyme in NE synthesis and a survey of its immunohistochemistry showed that many MITN receive substantial NEergic innervation (Vogt et al. 2008). In addition, many of these nuclei are nociceptive and project to cingulate cortex suggesting that LC projections may modulate pain processing directly in thalamic neurons and cingulate cortex by increasing signal-to-noise in both regions. The role of the LC in modulating behavioral states has been reviewed by Berridge and Waterhouse (2003). Since LC neuron discharges tend to occur in large groups, it is unlikely that the details of responsivity during sensory–discriminative tasks with various cues and rewards, anticipatory responses and rapid-training reversal, are derived by information in LC. More likely, these responses result from the projections of cingulate cortex to the LC. Indeed, many of the anticipatory, reward coding, and response selection functions attributed to the LC have also been demonstrated in the cingulate gyrus. Even the role of the LC in the autonomic aspects of emotion (Aston-Jones et al. 1996) could be partially explained by projections from anterior cingulate area 25 to the LC.

There are direct and reciprocal connections between NEergic systems and the cingulate gyrus associated with mutual information processing including pain and stress alterations. The descending cingulate projections to the LC have been shown in monkey and cat (Chiba et al. 2001; Room et al. 1985) and nociceptive midcingulate cortex (MCC; Vogt 2005) is in a position to drive the LC. Lesions of ACC block gastric ulcers caused by restraint stress in rats (Henke 1983) and intermittent footshock and restraint stress enhance expression of the immediate early protein cfos in anterior cingulate cortex (ACC) area 32 (Sawchenko et al. 2000; Rosene et al. 2004). Nociceptive afferents are a major input to the LC from the paragigantocellular nucleus of the reticular formation (PGi) since lidocaine block of PGi blocks nociceptive activation of the LC (Ennis and Aston-Jones 1988; Ennis et al. 1992). The MITN are a primary source of nociceptive information to ACC and MCC (Vogt

et al. 1979, 1987; Vogt 2005) but nothing is known of how the LC modulates thalamocingulate neuronal activation during noxious and stress stimulation. The extent to which each nociceptive nucleus in the thalamus projects to cingulate cortex needs to be evaluated in the context of LC projections, that is, DBH-ir axons in the MITN.

A key MITN that may mediate nociceptive and stress-mediated responses is the parafascicular nucleus (Pf). The Pf is nociceptive (Casey 1966; Dong et al. 1978) and it receives cingulate (Chiba et al. 2001; Room et al. 1985; Yasui et al. 1985) and LC (Jones and Yang 1985) inputs. The Pf likely contributes to descending pain control, since it projects to the periaqueductal gray (Sadikot et al. 1992) and electrical stimulation of the Pf generates mainly excitatory responses therein as does noxious heat or pressure stimulation of the skin (Sakata et al. 1988). Nociceptive afferents are transmitted from the spinal cord (Willis et al. 1979; Apkarian and Hodge 1989), subnucleus reticularis dorsalis (SRD; Bernard et al. 1990; Villanueva et al. 1998) and the parabrachial (Royce et al. 1991; Bester et al. 1999; Pritchard et al. 2000) nuclei to the MITN and each of these nuclei project in turn to cingulate cortex (Minciacchi et al. 1986; Royce et al. 1989). The following nuclei receive spinothalamic afferents and have been reported to contain nociceptive neurons (above and Ammons et al. 1985) and project to cingulate cortex: Pf, centrolateral (Cl), paracentral (Pcn), reuniens (Re), paraventricular (Pv), central, ventromedial (VM), parvocellular mediodorsal (MDpc), and limitans (Li). In addition, the parabrachial nucleus and SRD contain nociceptive neurons and project to Re, Pf, VM (Menendez et al. 1996; Pritchard et al. 2000; Villanueva et al. 1988, 1998) and, as noted, each of them project to cingulate cortex. Evidence of direct nociceptive transmission via MITN arises from lidocaine injections into the Pf that block such activity (Sikes and Vogt 1992).

There appear to be only two nuclei that project NEergic axons to the thalamus including the LC and A1/A5. The latter nucleus receives a cardiovascular input, primarily a heart rate signal from baroreceptors, and projects to the Pv nucleus of thalamus (Byrum and Guyenet 1987; Woulfe et al. 1990). Since the LC also projects to Pv (Jones and Yang 1985), it cannot be concluded that all DBH activity in Pv arises from the LC. As no other thalamic nuclei receive A5 inputs, the DBH to the remainder of the MITN likely arises entirely from the LC.

The above observations lead to the conclusion that, in addition to a broad and diffuse projection to most parts of the forebrain, the LC likely has preferential inputs to the mediodorsal and MITN, it is nociceptive, and it regulates thalamocingulate projections involved in nociceptive processing. The hypothesis for this study led us to evaluate the "hot spots" of LC projection targets using DBH immunohistochemistry. Nuclei with either moderate or dense DBH innervation were considered in detail including a number of other structural characteristics such as calcium-binding proteins and intermediate neurofilaments. Seven MITN stand out along with MD with dense LC input, nociceptive responses, and projections to cingulate cortex: Li, Pf, Pv, Re, Cl, Csl, and Cs.

Methods

Ten adult, cynomolgus monkeys were anesthetized with an excess of sodium pentobarbital and perfused via intracardial perfusion with 100 ml cold saline followed by 1 l of cold, 4% paraformaldehyde over a period of 45 min. All procedures involving the handling of animals were approved by the Committee for the Humane Use of Animals at SUNY Upstate Medical University. The brains were removed, the hemispheres separated, and each one bisected in the coronal plane, and digitally photographed. The brains or thalami were cut in a cryostat into six series at 40 μm thickness. Floating sections were pretreated with 75% methanol/25% peroxidase, followed by a 3 min pretreatment with formic acid (NeuN only) and then a washing with distilled water and two washes in phosphate buffered saline (PBS). Sections were incubated in primary antibody in PBS (dilutions: SMI32, 1:10,000, mouse; NeuN, Chemicon, Temecula, CA, 1:1,000, mouse; calbindin, Chemicon, 1:2,500, goat; DBH, Chemicon, 1:500, sheep) containing 0.3% Triton X-100 and 0.5 mg/ml bovine serum albumin (BSA) overnight at 4°C. The SMI32 antibody (Sternberger Monoclonals, Luthersville, MD) is to non-phosphorylated epitopes on the middle and heavy subunits of the neurofilament triplet. Sections were rinsed in PBS and incubated in biotinylated secondary antibody at 1:200 in PBS/Triton-X/BSA for 1 h. Following rinses in PBS, sections were incubated in ABC solution (1:4; Vector) in PBS/Triton-X/BSA for 1 h followed by PBS rinses and incubation in 0.05% diaminobenzidine, 0.01% H_2O_2 in a 1:10 dilution of PBS for 5 min.

After final rinses in PBS, sections were mounted, air-dried, counterstained with thionin, dehydrated and cover slipped. None of the DBH sections were counterstained with thionin. The reaction specificity was evaluated by excluding the primary antibody from the reaction or by including a peptide blocker (calbindin) to block the reaction. Most sections were counterstained to assure that nuclei and layers with high immunoreactivity are so stained and could be localized to individual MITN which are often quite narrow and interspersed among many other nuclei along the midline and the medial medullary lamina. Thus, the NeuN-ir, SMI32-ir, and calbindin-ir sections were stained for 3 min in thionin (0.05%, 3.7% sodium acetate, 3.5% glacial acetic acid, pH 4.5).

The nomenclature follows Olszewski's (1952) analysis of the monkey thalamus. It was further modified to express nuclear differences in DBH and calcium-binding protein observations and his VLm is termed VM according to current usage. Lower case abbreviations are used for fiber tracks.

The survey refers to three levels of DBH activity because those nuclei with moderate or high levels of activity are the primary focus of study. Other antibodies are used to identify nuclei and subnuclei in the mediodorsal and MITN based on this assessment. Examples of low, moderate, and high density DBH immunoreactivity is shown in black and white in Fig. 5d–f for three nuclei in the same section. The low level activity is overlooked as part of a general, and possibly, non-selective NEergic projection system as it appears everywhere in the brain except the caudate nucleus. In contrast, the moderate and high levels of DBH activity are emphasized as providing significant regulation of particular nuclei. Microdensitometry was performed on some nuclei to verify a quantitative link with the three qualitative levels as shown in Fig. 5d–f where the three blue rectangles indicate the sampling sites in each nucleus. The Bioquant Densitometry tool (Nashville, TN) was used with a 43,200 μm^2 rectangle to evaluate the area in μm^2 of thresholded DBH+ axons. The following mean ± SEM values were determined: light 3,871 ± 188, moderate 5,356 ± 1,032, heavy 15,586 ± 3,210.

The analytical approach involved taking low magnification digital photographs (10–40×) of DBH preparations for each case with the MacroFire camera (MicroBrightField, Williston, VT). These were used to identify nuclei with moderate or high levels of activity at higher magnification (100–200×). These latter nuclei were then evaluated at the same magnification for the other antigens in adjacent sections. The digital photographs were imported into different layers in Photoshop CS2 and coregistered using identifiable blood vessels and surface features where available as the ventricular ependyma. The borders of each nucleus were outlined in the NeuN and DBH sections and there were merged. Small adjustments often had to be made to match adjacent sections for a number of reasons; sometimes even a 0.25 mm distance between sections had a profound influence on the size and shape of a nucleus particularly in the posterior thalamus. One example is in Fig. 4 where the dorsal DBH site (a, shown in red) had to be extended medially to accommodate the paraventricular nucleus (Fig. 4b). This assured that the locations of NeuN, CB, and CR neurons were accurately identified in each subdivision of each nucleus. Finally, fitting DBH terminations to small intranuclear groups of neurons can only be done in a limited way. The details of intranuclear coregistrations will require double labeling and electron microscopic studies based on hypotheses generated by these observations.

Results

An overview of nine coronal levels through the thalamus for DBH-immunoreactive (DBH-ir) axonal plexi is shown in Fig. 1. They begin with the largest and most dense plexus in a confluence of nuclei in the posterior thalamus. The levels are numbered (1., 2.) throughout the text as each figure considers different levels from Fig. 1, while sections of each figure are labeled with capital letters. The confluence in the first two sections includes the most posterior limitans nucleus (Li) and densocellular division of the mediodorsal nucleus (MDdc). These nuclei are shown at a higher magnification and include a NeuN preparation to show the densely packed neurons of limitans just dorsal to the pretectal region. Although all thalamic nuclei have at least a low level of DBH-ir axons, the present assessment emphasizes nuclei with moderate or high levels of DBH activity. These three levels of enzyme activity are shown in black and white in Fig. 5, so the color processing does not detract from the full range of immunoreactivity, particularly at low levels. These qualitative levels are linked quantitatively to immunoreactive axons using microdensitometry (see "Methods").

At level 2 in Fig. 1, the habenulointerpeduncular tract is seen just before it penetrates the habenula. Medial to this tract is the most dense DBH activity in the parafascicular (Pf) and paraventricular (Pv; asterisk) nuclei. The next level 3 has a dense, DBH-ir fiber bundle that is part of and lateral in the habenulointerpeduncular tract. This appears to be one of the major pathways entering the thalamus and the habenulointerpeduncular tract is not a habenular efferent pathway only. A subsequent level of the thalamus contains dense plexi including the following nuclei in the caudal-to-rostral orientation: Cl, mediodorsal magnocellular (MDmc), superior centrolateral (Csl), central inferior (Cif), Re, multiformis division of MD (MDmf), parataenial (Pt), and superior central (Cs).

The high density of DBH-ir axons in Pf in level 2 is of particular interest because a similar level of activity is not present lateral to the habenulointerpeduncular tract. It is also adjacent to axons in the Pv and forms a complex pattern; that is, the projection to Pf, even in the medial part, is not uniform. A more detailed analysis of level 2 is in Fig. 2 where it is clear that the Pf is not uniform in terms of the size and density of neurons. It appears that the DBH-ir axons select between two parts of Pf medial to the habenulointerpeduncular tract; the medial part of Pf (Pfm) is comprised of neurons with dense levels of DBH-ir axons, while the other division does not receive this input and

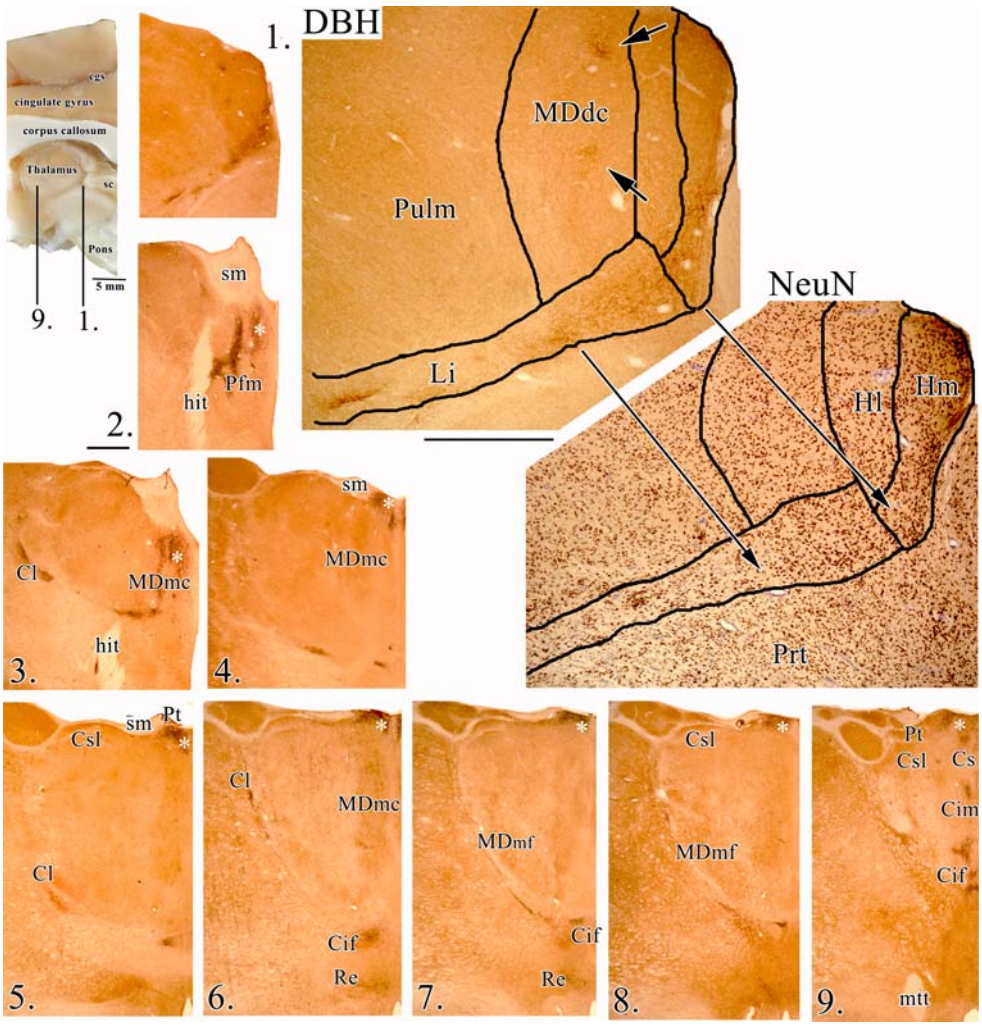

Fig. 1 Overview of DBH immunoreactivity in thalamus. The nine levels are shown with the medial surface and numbered by coronal section, and these numbers are used in subsequent figures. The most dense and largest concentration of DBH-ir axons is in sections *1* and *2* and that for *1* is magnified and the nuclei outlined to demonstrate the location of the Li and a few patches in MDdc and a coregistered section of NeuN immunhistochemistry to show the Li (*arrows*). The Pv is labeled in each section with a *white asterisk* and DBH activity in the habenula is not considered; other thalamic nuclei with moderate or high DBH-ir are labeled in the low magnification sections. *cgs* Cingulate sulcus, *hit* habenulointerpeduncular tract, *Hl* lateral habenula, *Hm* medial habenula, *Prt* pretectal area, *sc* superior colliculus. *Magnification bars* are 200 μm

there is a greater variability in neuron sizes; therefore, the latter is termed multiformis (Pfmf). The calcium-binding proteins are primarily expressed in Pfm and not Pfmf (Fig. 2c, d, f, g), although not all of the neurons even in Pfm express calbindin (CB) or calretinin (CR) and a further subdivision of Pfm may become necessary as the DBH+ plexus does not appear in the medial part of Pfm.

The density of neurofilament protein expression also differentiates Pfm and Pfmf. Figure 3 shows SMI32 immunoreactivity in three cases; case 1 (Figs. 1 and 2) and cases 2 and 3 in Fig. 3. Case 1 in Fig. 3 is thionin counterstained and Pfmf shows high expression of NFP, while there is a low level of NFP in Pfm. Coregistration of the NeuN section at a similar level shows neurons in Pfm and the multiple sizes of neurons in Pfmf. The dispersion of Pfmf may explain some of the "gaps" in DBH labeling in the medial part of Pf but double-labeling studies will be needed to verify this. Cases 2 and 3 are shown at lower magnification and higher magnifications to emphasize that the lateral division of Pf (Pfl) also has a low level of NFP expression. Thus, the heterogeneity in DBH-expressing axons in the Pf is due to its selection of a subdivision of Pf rather than a simple projection to the entire nucleus, both laterally and medially.

The MITN preference of the DBH-ir axons is well demonstrated in Fig. 4 where they can be seen around and in the mediodorsal nucleus. The plexus is shown in Cl and is coregistered to NeuN, SMI32, and CB-ir and shows again that the high density of DBH-ir axons is associated with low levels of neurofilament proteins and high levels of calcium-binding proteins. The MDmc at this level has a high density of DBH-ir axons and this plexus extends into the Pv. The Pfm has low DBH-ir axons and CB-ir neurons in contrast to the heavily stained Cl.

The distribution of DBH-ir in and around the mediodorsal nucleus is further shown in Figs. 5, 6, 7, and 8. A middle level of MDmf is in Fig. 5 that has a moderate density of DBH-ir axons and little CB-ir in contrast to Cl, Csl, Pv, and Cim that have a high level of both. At a more rostral level of the thalamus (#6 in Fig. 1), the border

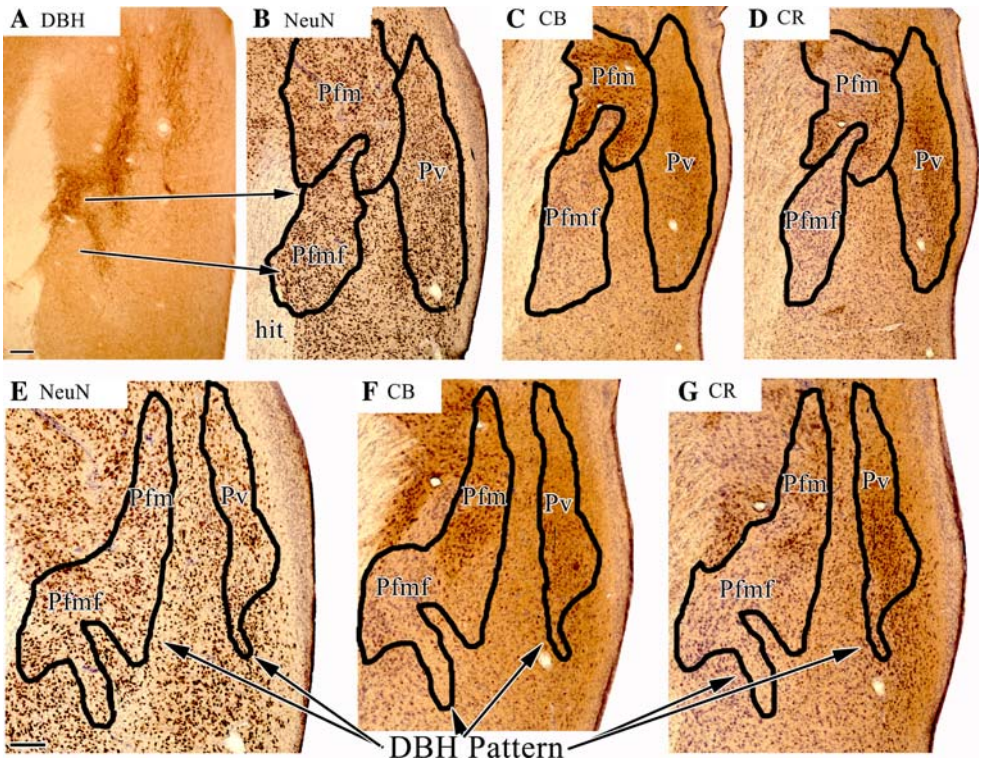

Fig. 2 Adjacent sections show the distribution of DBH, NeuN, and the calcium-binding proteins (CB and CR) in the medial (Pfm) and multiformis (Pfmf) divisions of Pf. Sections **b–d** were magnified by 50% in **e–g** and the DBH pattern (*black outline*) coregistered to show the extent of overlap of this projection with divisions of Pf and Pv. *Magnification bars* are 200 μm

between MDpc and MDmc is magnified in Fig. 6. Here the moderate density of axons in MDmc and low density in MDmf and MDpc is apparent. Although the CB reaction product is highest in Csl, Cl, Pt, and Pv, it is also present at a moderate level throughout MD that cannot be appreciated at low magnification when the sections are counterstained. The counterstaining was used to assure a correct identification of immunoreactivity in the MITN.

Figure 7 photographs are located ventral to that in Fig. 6 and in level #6 in Fig. 1. Here the moderate density of DBH-ir axons in MDmc is seen as well as the higher density of such axons in Cif and Re. Neither the Pcn or VM has anything more than a low density of DBH-ir axons. To the extent that VM has nociceptive activity and projects to cingulate cortex, this suggests a different role of such projections in pain processing as discussed below. The highest density of CB-ir neurons is in the Cim, Cif, and Re nuclei with lower numbers of CR+ neurons in the same nuclei. A low density of CB-ir neurons is also in the Pcn, and MDmc nuclei.

The most rostral level #9 of the thalamus is in Fig. 8. Of particular note at this level is the high density of DBH-ir axons in MDmf that was not present caudally. As this is not characteristic of most parts of the nucleus, we refer to this as MDmfa for "anterior". It also appears there is a moderate level of activity in Pcn. The continued heavy DBH labeling in Csl, Cs, Pv, and Pt are also present. Another difference of the MDmfa with its caudal counterparts is the high density of heavily labeled CB-ir neurons. These observations are documented at a higher magnification, as is the difference in cytoarchitecture between MDmfa and Pcn in Fig. 8. This includes the high number of CB-ir neurons (Fig. 8g).

Discussion

Immunoreactive DBH axons were usually associated with CB-ir and CR-ir neurons and low levels of neurofilament proteins in the mediodorsal and MITN. The paraventricular, superior centrolateral, limitans and central nuclei had relatively high and evenly distributed DBH, while the mediodorsal magnocellular and paracentral nuclei had a moderate and even distribution. Heterogeneities in DBH-ir in other nuclei raise questions of functional segregation. The anterior multiformis part of the mediodorsal nucleus, but not middle and caudal levels, had high activity. The posterior parafascicular nucleus was heterogeneous; the lateral part had little DBH activity, its medial division a high level, and its multiformis part only a small amount. To the extent that many of these thalamic nuclei are nociceptive and the LC is active during stress, nuclei in the MD and MITN that receive a high level of NEergic input may provide important sites of interactions between pain and "stress" (fight-or-flight) circuits. The Pv receives dense and

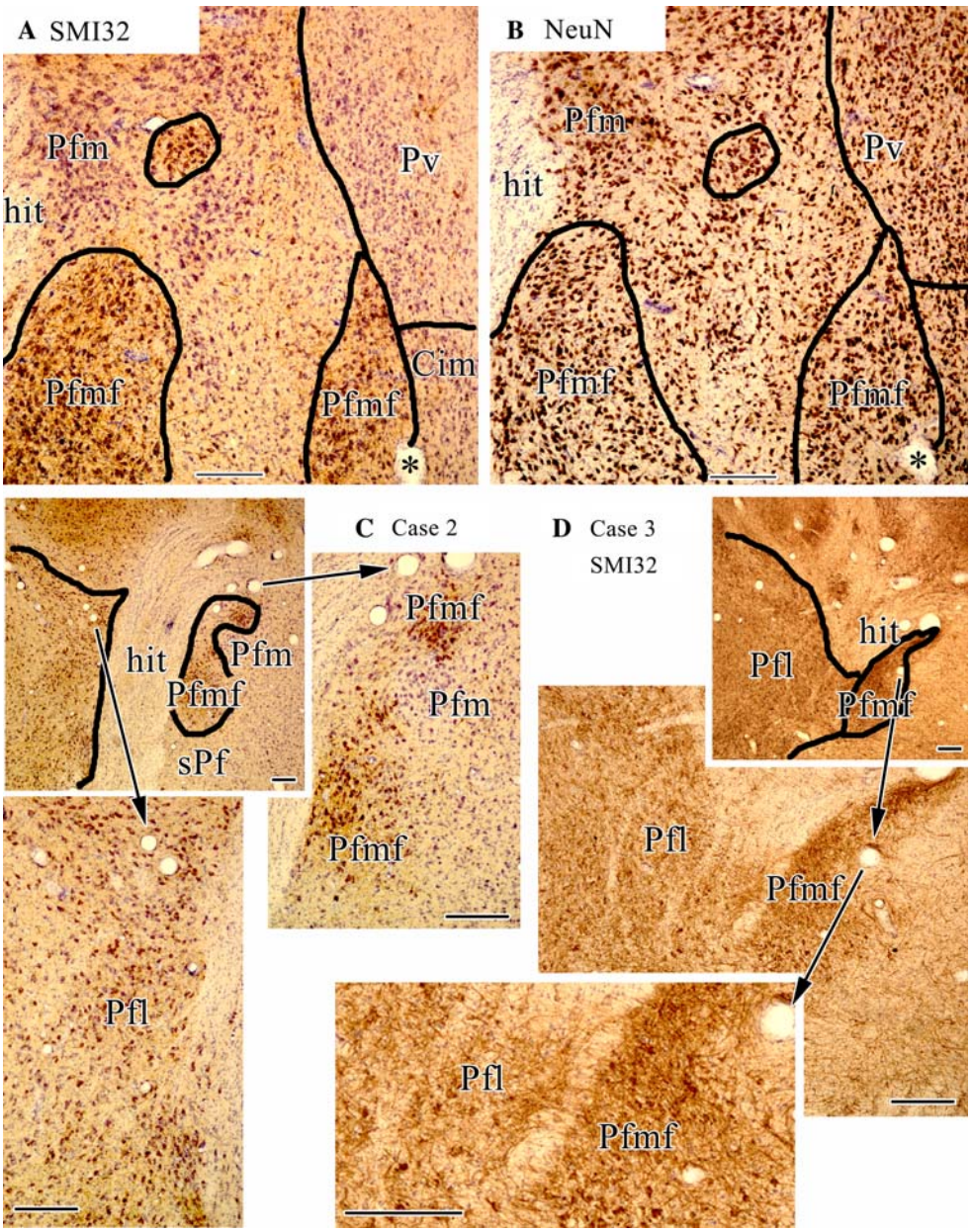

Fig. 3 Pfmf is characterized by neurons that express high levels of intermediate neurofilament proteins (SMI32), while Pfm neurons do not. The variability of neuronal sizes in Pfmf is clear with the NeuN preparation (*asterisks* identify common blood microvessels) when compared to the Pv that contains uniformly small neurons and the Pfm that has primarily moderate-sized neurons. **c** Pfmf heavy CB-ir neurons, while Pfl and sPf have few such neurons. **d** Low magnification of the SMI32 antibody for case 3 shows that Pfmf has very high expression, while that in Pfl has much less though still abundant neurofilament proteins. All *calibration bars*: 200 μm

homogeneous DBH afferents and it has both baroreceptor- and nociceptive-coded information.

Interactions of cingulate cortex and LC

It is a striking fact that some neuron functions in cingulate cortex have been demonstrated in the LC and these are likely subserved by their reciprocal connections. Of course, some of the functions of cingulate cortex, including long-term and working memories, decision-making, and conflict resolution cannot be performed by LC. Simple functions, however, such as attending to targets, and responding to noxious stimuli are shared by both of these structures. While LC neurons have decreased activity during sleep and automatic behaviors such as grooming and eating, there are two waking, behavioral states with unique LC neuron discharge properties (Aston-Jones et al. 1999). In the *phasic mode* of firing, there is a moderate level of tonic discharge and phasic LC activation facilitates behavioral responses to target stimuli with short-LC responses. Phasic activation appears to code the meaning or salience of the reward properties of a stimulus and not other aspects of the task including sensory attributes, target frequency, lever release, fixation spot or non-target (context) stimuli (Aston-Jones et al. 1997). During the *tonic mode* of firing, LC neurons have high ongoing activity during poor task

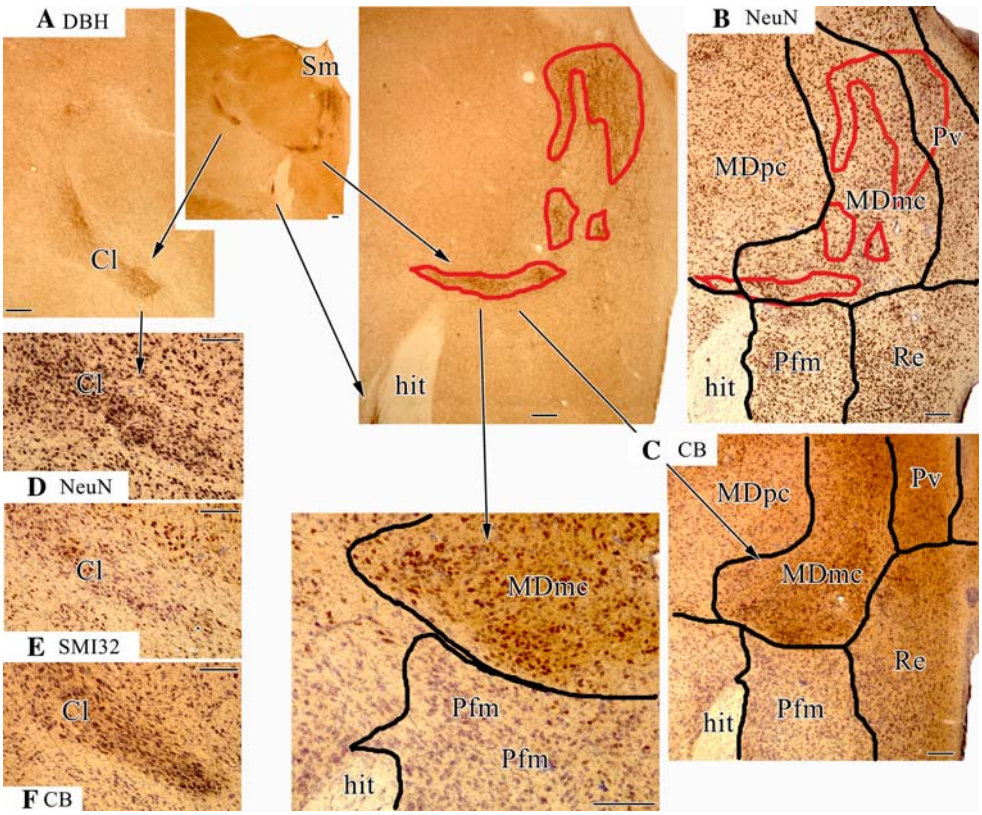

Fig. 4 Details of DBH immunohistochemistry at level #3 (Fig. 1) and coregistration to other antibodies. The four aggregates of DBH-ir are outlined in *red* (**a**) and transferred to the NeuN section (**b**) with a slight extension into Pv. Though patchy, most of the label is in MDmc. The heavy DBH labeling in Cl and MDmc is shown, as is heavy CB-ir, in both nuclei. **c** Contains two magnifications of CB in this region. All *calibration bars* are 200 μm

performance, and weak and poorly discriminative phasic responses to sensory stimuli during visual-discrimination testing. This is a state of high arousal and sensory scanning rather than high-resolution behavioral performance and this state may be pivotal to the role of cingulate cortex in evaluating behavioral solutions in novel situations.

Shifting between LC firing modes provides two different types of behavioral output that are linked to cingulate functions (Aston-Jones et al. 1996, 1999). During phasic discharges, processing of specific sensory cues is efficient as the animal's attention to behavioral output is coupled, possibly directly, to MCC outputs because this region regulates detailed skeletomotor functions. During the tonic mode of LC firing, sensory processing and links to particular sensory stimuli are weak and the high tonic discharge rate may be adaptive to changing or unpredictable outcomes and more responsive to unexpected events. In this instance, the LC may be disengaged from MCC and more profoundly engaged with subgenual ACC that mediates general autonomic activation and reflexive orienting.

Noxious footshock stimulation is particularly effective in driving LC output during the tonic mode of firing (Chang and Aston-Jones 1993; Ennis et al. 1992). MCC driving or coordination of LC activity is likely high during phasic and low during tonic modes of firing and the former involves detailed sensory inputs, cingulate driving, and accurate behavioral output. In contrast, the tonic mode is a state of high arousal and lacks sensory details as shown with target detection, and a higher correlation of discharges is possible with ACC. Thus, a functional circuit for cingulate-mediated, sensorimotor processing occurs during phasic-mode LC firing and is disengaged during tonic-mode firing.

Nociceptive driving of LC and cingulate cortex

LC neurons discharge during slowly conducting, C-fiber activation associated with the burning aspect of pain, an effect that can be blocked by injection of capsaicin directly into the sciatic nerve (Hirata and Aston-Jones 1994). Peristimulus–time histograms show robust discharges over baseline following footshock that resolve into two components: an excitatory output and a secondary inhibitory component. Although some lamina I spinal afferents terminate directly in the LC (Westlund and Craig 1996), the main source of nociceptive excitation of LC neurons appears to be the PGi (Ennis and Aston-Jones 1988; Ennis et al. 1992). Electrical stimulation of PGi or kainate receptor agonists drive activity of LC as does footshock stimulation, while blockade of these receptors in PGi prevented the activation of LC neurons by noxious

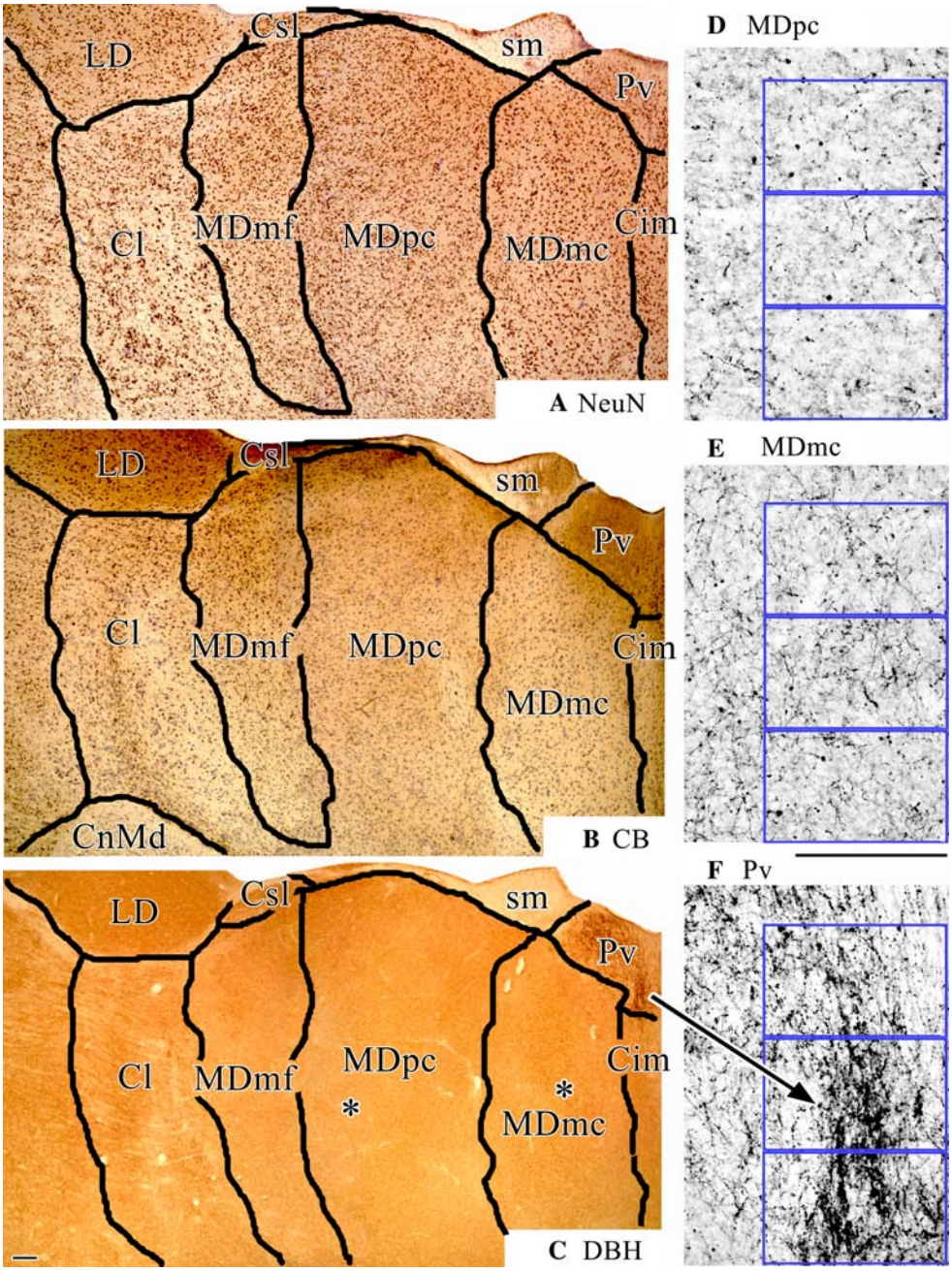

Fig. 5 Cytoarchtitecture and DBH immunoreactivity at level #4 (Fig. 1). The Csl, Cl, Pt, Cs, Pv, and Cim have dense DBH-ir axons and CB-immunoreactive neurons. Although MDmf has significant DBH-ir, there is limited CB reactivity that differs considerably at posterior levels of this nucleus. The *black and white images* in **d**–**f** show the three essential levels of DBH immunoreactivity referred to throughout this study. The overlying *blue* rectangles in each section are the target sites used for microdensitometry and determine equivalents of light, moderate, and dense immunoreactivity. The *asterisks* in **c** show the points at which **d** and **e** were sampled, respectively, while the *arrow* to **f** shows the part of Pv magnified for the comparison. Both *calibration bars* are 200 μm

footshock and the source of nociceptive input to PGi likely arises in the spinal cord (Abols and Basbaum 1981; Menetrey et al. 1983). Thus, acute noxious stimulation drives spinal inputs to the PGi and these are transmitted to the LC in an excitatory pathway (Aston-Jones et al. 1993). These spinal nociceptive afferents are projected further into the MITN and from there, to drive the ACC and MCC (above). Thus, both the LC and cingulate cortex are jointly and powerfully driven by noxious stimulation and such activity converts LC neuronal discharges to the tonic, search mode. One possible consequence of this state is that limbic motor systems are coordinated throughout the forebrain and midbrain in a search for predictive cues to use for avoidance of future nociceptive stimulation and enhancing of memories associated with the event in the forebrain.

MITN as nociceptive gateway to limbic motor systems

Although all thalamic nuclei receive some NEergic input, there are a few particularly heavily innervated MITN and this provides for important circuit interactions between

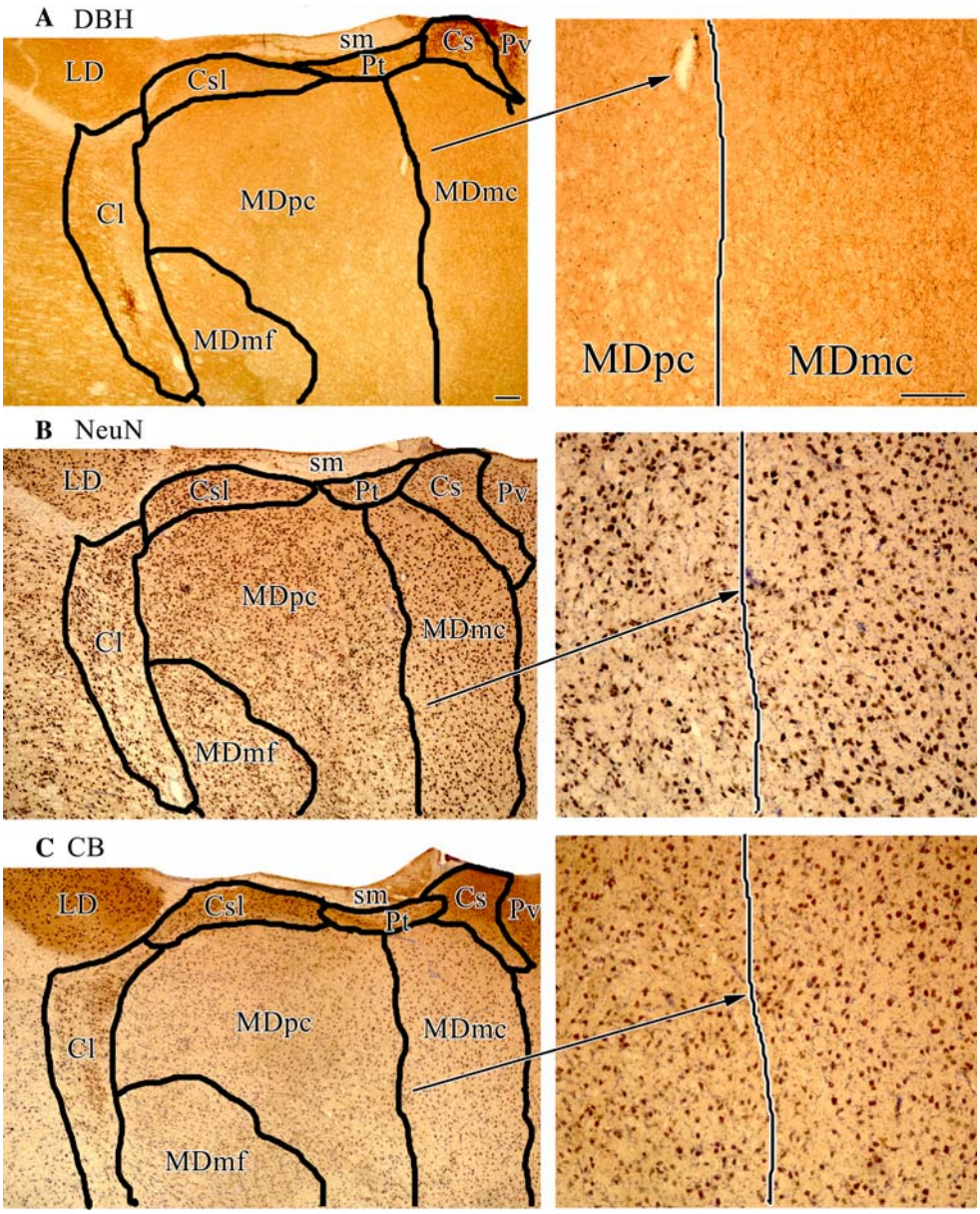

Fig. 6 The border between MDpc and MDmc at two magnifications; *arrows* show the origin of higher magnification photographs. Both MDmc and MDmf have a moderate level of DBH immunoreactivity, while heavy plexi are in Cl (though not uniformly high), Cs, Csl, Pt, and Pv. The larger neurons in MDmc are shown in **b** *NeuN*. There seems to be a light CB immunoreactivity throughout much of MD that is not apparent at lower magnifications when a counterstain is present. Both *calibration bars* are 200 μm

cingulate and NEergic systems. Particular thalamic nuclei might be viewed as pain portals that can be modified by activity in the A5 and LC and they may be preferentially vulnerable to nociceptive driving in chronic stress syndromes. Certainly, interaction of subgenual ACC with NEergic systems in the lateral parabrachial nucleus provide another site critical for visceral nociceptive interactions. Nociceptive MITN that project to cingulate cortex include the Pf, Cl, Pcn, Re, Pv, Ce, VM, MDpc, and Li. All of these nuclei but the Pcn and VM have high levels of DBH activity. Thus, the following nociceptive nuclei that project to cingulate cortex receive NEergic inputs in descending order for density of DBH-ir axons: MDpc, Li, Pfm, Pv, Cl, Ce, Re. It appears that NEergic afferents are at a pivotal point in many MITN to modulate nociceptive activity *before* it arrives in midcingulate cortex. This could result in longer duration responses and enhance the chance that cingulate plasticities associated with recall of past events, response selection, and memory storage is enhanced.

Cardiovascular afferents

One of the highest densities of DBH-ir axons is throughout the Pv nucleus, which receives both A5 (Byrum and Guyenet 1987) and LC inputs (Comans and Snow 1981; Jones and Yang 1985). Dual inputs throughout the CNS are

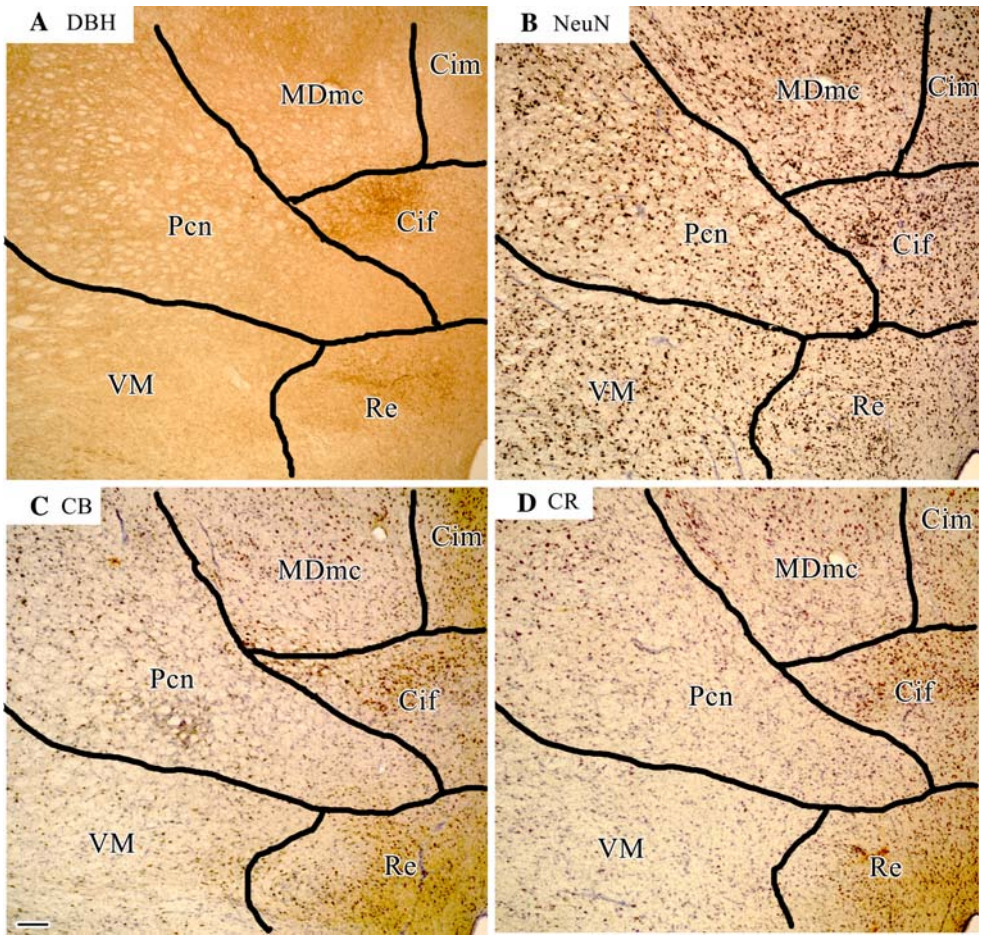

Fig. 7 A ventral part of the medial thalamus from the level shown in Fig. 6. The high density of DBH axons in Cif and Re are shown along with CB- and CR-immunoreactive neurons in the same nuclei. *Calibration bar* is 200 μm

mediated by NEergic nuclei in the brainstem: cardiovascular and nociceptive. The cardiovascular inputs arrive in the A1/A5 nuclei and LC from the caudal nucleus of the solitary tract. The A1 and A5 NEergic nuclei are primarily involved in baroreceptor responses and buffering sudden blood pressure changes. These nuclei provide a heart-rate signal for monitoring cardiovascular function and a means for descending systems to modify output according to ongoing behavioral needs. The A1 and A5 nuclei project to the lateral parabrachial, ventrolateral periaqueductal gray, central nucleus of the amygdala, and the MITN (Byrum and Guyenet 1987; Woulfe et al. 1990). Visceral input to these nuclei also arrives from the caudal part of the nucleus of the solitary tract (Beckstead et al. 1980). Since the rostral projections of A1 and A5 are NEergic and intermingle with LC projections, projections to the Pv, the DBH preparations to the MITN must be viewed as a common input from A1, A5, and the LC. Finally, the common activation of this system by nociceptive and visceral afferents assures synchronization of NEergic and cingulate system functions including behavioral states associated with LC neuron discharges. The joint innervation of cardiovascular and nociceptive systems by NEergic afferents via the MITN may coordinate their processing to assure they are both joined temporally and form part of a common memory substrate.

Extrapyramidal motor system connections and integrated circuit model

Thalamic nuclei that project to midcingulate cortex also project to the limbic striatum (Pandya et al. 1981) and the rich projections of the MITN to the striatum have been reviewed by Haber and Gdowski (2004). Kunishio and Haber (1994) showed that the cingulate gyral surface and sulcal premotor areas have distinct projections with rostral gyral and sulcal projections to limbic striatum and "sensorimotor" striatum, respectively. Of primary interest here is the fact that Pfm projects to the medial ventral striatum, also termed the limbic striatum in view of its many limbic cortical inputs. A crucial link between NEergic projections to the MITN and interactions with the limbic striatum can be made based on the pattern of DBH input and medial ventral striatal efferents.

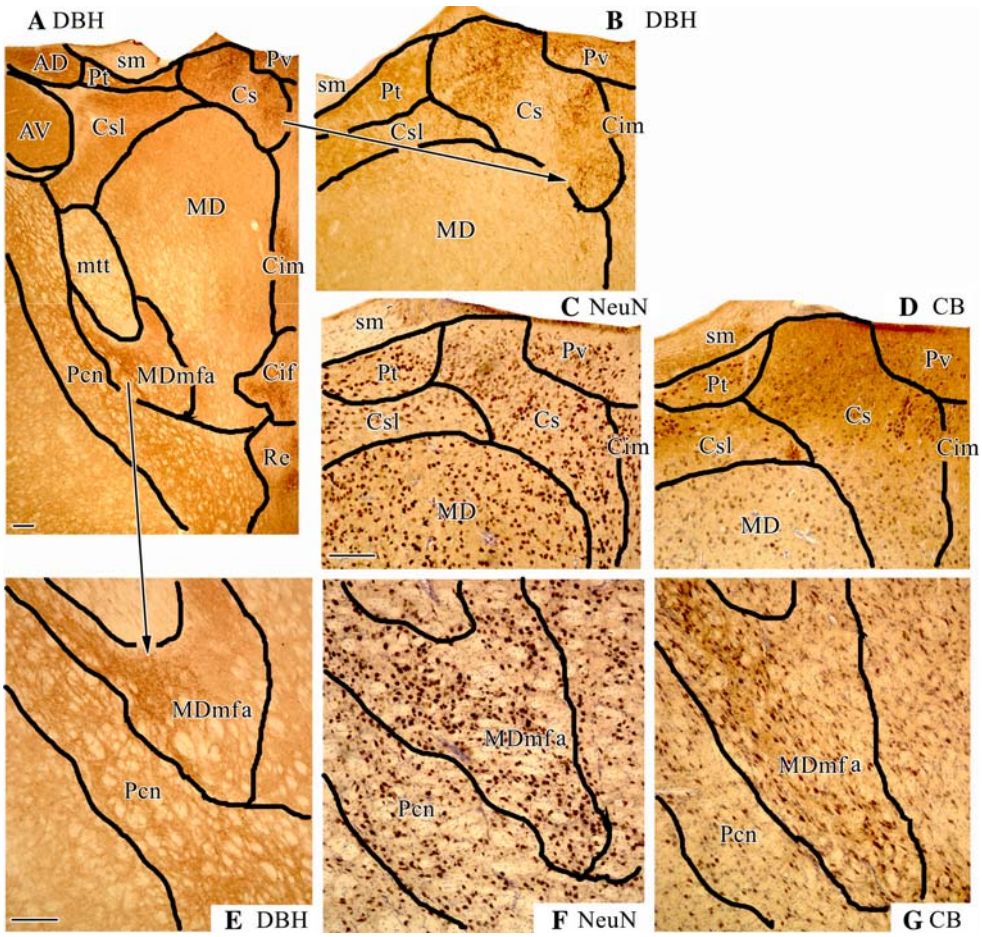

Fig. 8 A rostral level of the thalamus (#1 in Fig. 1) showing the dorsal midline nuclei and the particularly high density of DBH-ir axons and CB+ neurons in MDmfa. *mtt* Mammilothalamic tract. All *calibration bars* are 200 μm

Figure 9c provides a summary of the latter efferents from the medial PF and Pv (Giménez-Amaya et al. 1995). Indeed, the Pv labeling in both instances is extensive throughout the entire nucleus. It is an amazing fact that this output pattern matches the distribution of DBH-ir axons shown in Fig. 2. This suggests that rather than just regulating nociceptive sensory afferents through the thalamus to cingulate cortex, there may also be an important regulation of extrapyramidal motor systems by NEergic projections to the MITN. Interestingly, the lateral Pf projections of the rostral cingulate premotor area are particularly dense (Hatanaka et al. 2003), while those from the Pfm are dense to the adjacent gyral surface (Fig. 9a). This might be a key linkage between pain processing systems via the PFl and gyral cortex and skeletomotor output in the cingulate premotor systems and Pfm. Thus, although the details of skeletomotor output associated with nociceptive stimulation may be organized in MCC, NEergic innervation of the striatum could provide extrapyramidal motor support to enhance and focus such outputs as it coordinates emotional motor system outputs. Certainly, the limbic striatum must be viewed as a part of the limbic motor system.

The primary conclusion from the present study is that the NEergic inputs to the MITN regulate nociceptive processing through the thalamus and into cingulate cortex and they modulate skeletomotor outputs likely relevant to such sensory processing. The nociceptive afferents terminate in PGi and LC as well as the MITN (red arrows) as shown in Fig. 9d. The joint support of this system by LC output is shown in this figure with blue arrows. Jointly innervated MITN include the Pv, Csl, Cl, Re, Pf, and Li. Although these nuclei are generally viewed as nonspecific, they likely have some topographic specificity in projections to the cingulate cortex and this is shown for the ACC, MCC, and dorsal PCC regions based on earlier work (Vogt et al. 1987). Although there are many possible organizations for axon targeting and processing through these circuits, one likely scenario is that projections of Csl, Pv, and Pfm make the limbic striatal projections. The model in Fig. 9d, therefore, synthesizes the nociceptive input and skeletomotor output functions that are regulated by the LC/NEergic projection system. The joint regulation of key MITN by both nociceptive and LC afferents and their driving of limbic motor systems in cortex and the striatum are the critical conclusion of this analysis.

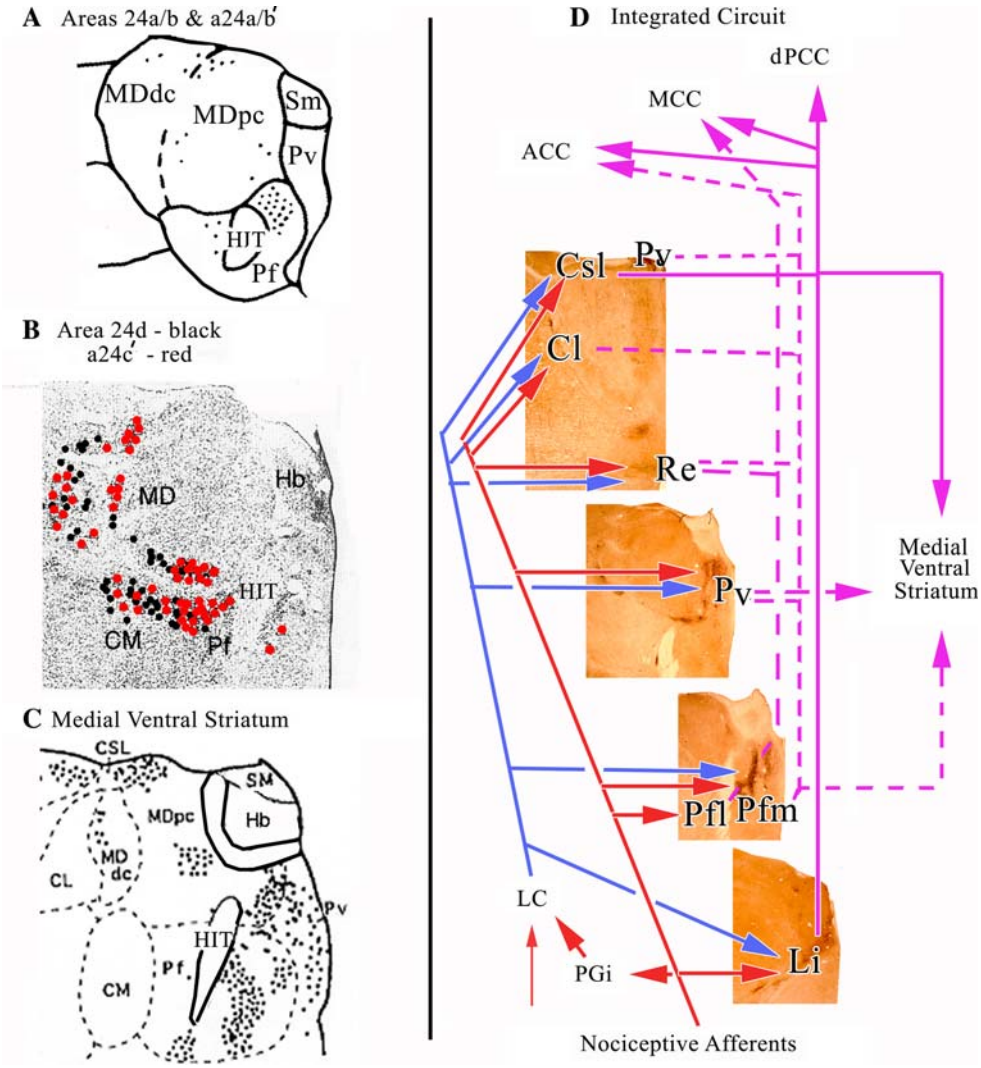

Fig. 9 Retrogradely labeled neurons in the MITN from injections in three sites. **b** ACC and MCC gyral surface (Vogt et al. 1987). **b** The cingulate motor areas in the cingulate sulcus (Hatanaka et al. 2003). **c** The medial and ventral striatum (Giménez-Amaya et al. 1995). The pattern of output to the medial ventral striatum noted in the latter study appears quite similar to that of the DBH innervation in Pf medial to the hit. **d** A circuit model of nociceptive afferents (*red*; *thin line* small input, *thicker line* main source) and their modulation by LC/NEergic afferents (*blue*) based on the MITN with the highest density of DBH-ir axons. Nociceptive afferents to dorsal PCC from the MITN that may be modulated by NE are shown with *solid purple arrows*, those to MCC are shown with *long dashes*, and those to ACC are shown with the *shortest dashes*. *Slightly thicker arrows* show projections into the medial ventral stratum and emphasize driving of the extrapyramidal system by projections from the MITN

Acknowledgments These studies were supported by the NIH-NINDS grant RO1-NS44222 (BAV) and the James S. McDonnel Foundation (220020078; PRH).

References

Abols IA, Basbaum AI (1981) Afferent connections of the rostral medulla of the cat: a neural substrate for midbrain–medullary interactions in the modulation of pain. J Comp Neurol 201:285–297

Abercrombie ED, Jacobs BL (1987) Single-unit response of noradrenergic neurons in the locus coeruleus of freely moving cats. I. Acutely presented stressful and nonstressful stimuli. J Neurosci 7:2837–2843

Ammons WS, Girardot M-N, Foreman RD (1985) T2–T5 spinothalamic neurons projecting to medial thalamus with viscerosomatic input. J Neurophysiol 54:73–89

Apkarian AV, Hodge CJ (1989) Primate spinothalamic pathways: III. Thalamic terminations of the dorsolateral and ventral spinothalamic pathways. J Comp Neurol 288:493–511

Aston-Jones G, Ennis M, Pieribone VA, Nickell WT, Shipley MT (1993) The brain nucleus locus coeruleus: restricted afferent control of a broad efferent network. Science 234:734–737

Aston-Jones G, Rajkowski J, Kubiak P, Valentino RJ (1996) Role of the locus coeruleus in emotional activation. Prog Brain Res 107:379–402

Aston-Jones G, Rajkowski J, Kubiak P (1997) Conditioned responses of monkey locus coeruleus neurons anticipate acquisition of discriminative behavior in a vigilance task. Neuroscience 80:697–715

Aston-Jones G, Rajkowski J, Cohen J (1999) Role of locus coeruleus in attention and behavioral flexibility. Biol Psychiatry 46:1309–1320

Beckstead RM, Morse JR, Norgren R (1980) The nucleus of the solitary tract in the monkey: projections to the thalamus and brain stem nuclei. J Comp Neurol 190:259–282

Bernard JF, Villenueva L, Carroue J, Le Bars D (1990) Efferent projections from the subnucleus reticularis dorsalis (SRD): a *Phaseolus vulgaris* leucoagglutinin study in rat. Neurosci Lett 116:257–262

Berridge CW, Waterhouse BD (2003) The locus coeruleus-noradrenergic system: modulation of behavioral state and state-dependent cognitive processes. Brain Res Rev 42:33–84

Bester H, Bourgeais L, Villanueva L, Besson J-M, Bernard J-F (1999) Differential projections to the intralaminar and gustatory thalamus from the parabrachial area: a PHA-L study in the rat. J Comp Neurol 405:421–449

Byrum CE, Guyenet PG (1987) Afferent and efferent connections of the A5 noradrenergic cell group in the rat. J Comp Neurol 261:529–542

Casey KL (1966) Unit analysis of nociceptive mechanisms in the thalamus of the awake squirrel monkey. J Neurophysiol 29:727–750

Chang C, Aston-Jones G (1993) Response of locus coeruleus neurons to footshock stimulation is mediated by neurons in the rostral ventral medulla. Neuroscience 53:705–715

Chiba T, Kayahara T, Nakano K (2001) Efferent projections of infralimbic and prelimbic areas of the medial prefrontal cortex in the Japanese monkey, *Macaca fuscata*. Brain Res 888:83–101

Comans PE, Snow PJ (1981) Ascending projections to nucleus parafascicularis of the cat. Brain Res 230:337–341

Devilbiss DM, Waterhouse BD (2004) The effects of tonic locus coeruleus output on sensory-evoked responses of ventral posterior medial thalamus and barrel field cortical neurons in the awake rat. J Neurosci 24:10773–10785

Dong WK, Ryu H, Wagman IH (1978) Nociceptive responses of neurons in medial thalamus and their relationship to spinothalamic pathways. J Neurophysiol 41:1592–1613

Ebert U (1996) Noradrenalin enhances the activity of cochlear nucleus neurons in the rat. Eur J Neurosci 8:1306–1314

Ego-Stengel V, Bringuir V, Shulz DE (2002) Noradrenergic modulation of functional selectivity in the cat visual cortex: an in vivo extracellular and intracellular study. Neuroscience 111:275–289

Ennis M, Aston-Jones G (1988) Activation of locus coeruleus from nucleus paragigantocellularis: a new excitatory amino acid pathway in brain. J Neurosci 8:3644–3657

Ennis M, Aston-Jones G, Shiekhatter R (1992) Activation of locus coeruleus neurons by nucleus paragigantocellularis or noxious sensory stimulation is mediated by intracoerulear excitatory amino acid neurotransmission. Brain Res 598:185–195

Foote SL (1997) The primate locus coeruleus: the chemical neuroanatomy of the nucleus, its efferent projections, and its target receptors. In: Bloom FE, Björklund A, Hökfelt T (eds) Handbook of chemical neuroanatomy: the primate nervous system, part I, vol 13. Elsevier, Amsterdam, pp 187–215

Giménez-Amaya JM, McFarland NR, De Las Heras S, Haber SN (1995) Organization of thalamic projections to the ventral striatum in the primate. J Comp Neurol 354:127–149

Ginsberg SD, Hof PR, Young WG, Morrison JH (1994) Noradrenergic innervation of vasopression- and oxytocin-containing neurons in the hypothalamic paraventricular nucleus of the macaque monkey: quantitative analysis using double-label immunohistochemistry and confocal laser microscopy. J Comp Neurol 341:476–491

Haber SN, Gdowski MJ (2004) The basal ganglia. In: Pxinos G, Mai JK (eds) The human nervous system. Elsevier, Sydney, pp 676–738

Hatanaka N, Tokuno H, Hamada I, Inase M, Ito Y, Imanishi M, Hasegawa N, Akazawa T, Nambu A, Takada M (2003) Thalamocortical and intracortical connections of monkey cingulate motor areas. J Comp Neurol 462:121–138

Henke PG (1983) Mucosal damage following electrical stimulation of the anterior cingulate cortex and pretreatment with atropine and cimetidine. Pharmacol Biochem Behav 19:483–486

Hirata H, Aston-Jones G (1994) A novel long-latency response of locus coeruleus neurons to noxious stimuli: mediation by peripheral C-fibers. J Neurophysiol 71:1752–1761

Jones BE, Yang T-Z (1985) The efferent projections from the reticular formation and the locus coeruleus studied by anterograde and retrograde axonal transport in the rat. J Comp Neurol 242:56–92

Kunishio K, Haber SN (1994) Primate cingulostriatal projection: limbic striatal versus sensorimotor striatal input. J Comp Neurol 350:337–356

Menendez L, Bester H, Besson JM, Bernard JF (1996) Parabrachial area: electrophysiological evidence for an involvement in cold nociception. J Neurophysiol 75:2099–2116

Menetrey D, Roudier F, Besson JM (1983) Spinal neurons reaching the lateral reticular nucleus as studied in the rat by retrograde transport of horseradish peroxidase. J Comp Neurol 220:439–452

Morrison JH, Foote SL (1986) Noradrenergic and serotoninergic innervaqtion of cortical, thalamic, and tectal visual structures in Old and New World monkeys. J Comp Neurol 243:117–138

Minciacchi D, Bentivoglio M, Molinari M, Kultas-Ilinsky K, Ilinsky IA, Macchi G (1986) Multiple cortical targets of one thalamic nucleus: the projections of the ventral medial nucleus in the cat studied with retrograde tracers. J Comp Neurol 252:106–129

Olszewski J (1952) The thalamus of the *Macaca mulatta*. S. Karger, Basel

Pandya DN, Van Hoesen GW, Mesulam M-M (1981) Efferent connections of the cingulate gyrus in the rhesus monkey. Exp Brain Res 42:319–330

Pritchard TC, Hamilton RB, Norgren R (2000) Projections of the parabrachial nucleus in the old world monkey. Exp Neurol 165:101–117

Room P, Russchen FT, Groenewegen HJ, Lohman AHM (1985) Efferent connections of the prelimbic (area 32) and the infralimbic (area 25) cortices: an anterograde tracing study in the cat. J Comp Neurol 242:40–55

Rosene DL, Lister JP, Schwagerl AL, Tonkiss J, McCormick CM, Galler JR (2004) Prenatal malnutrition in rats alters the c-Fos response of neurons in the anterior cingulate and medial prefrontal region to behavioral stress. Nutr Neurosci 7:281–289

Royce GJ, Gracco BC, Beckstead RM (1989) Thalamocortical connections of the rostral intralaminar nuclei: an autoradiographic analysis in the cat. J Comp Neurol 288:555–582

Royce GJ, Bromley S, Gracco C (1991) Subcortical projections to the centromedian and parafascicular thalamic nuclei in the cat. J Comp Neurol 306:129–155

Sadikot AF, Parent A, Francois C (1992) Efferent connections of the centromedian and parafasciculartha lamic nuclei in the squirrel monkey: a PHA-L study of subcortical projections. J Comp Neurol 315:137–159

Sakata S, Shima F, Kato M, Fukui M (1988) Effects of thalamic parafascicular stimulation on the periaqueductal gray and adjacent reticular formation neurons. A possible contribution to pain control mechanisms. Brain Res 451:85–96

Sawchenko PE, Li H-Y, Ericsson (2000) Circuits and mechanisms governing hypothalamic responses to stress: a tale of two paradigms. Prog Brain Res 122:61–78

Sikes RW, Vogt BA (1992) Nociceptive neurons in area 24 of rabbit cingulate cortex. J Neurophysiol 68:1720–1732

Villanueva L, Bouhassira D, Bing Z, Le Bars D (1988) Convergence of heterotopic nociceptive information onto subnucleus reticularis dorsalis neurons in the rat medulla. J Neurophysiol 60:980–1009

Villanueva L, Debois C, Le Bars D, Bernard J-F (1998) Organization of diencephalic projections from the medullary subnucleus reticularis dorsalis: a retrograde and anterograde tracer study in the rat. J Comp Neurol 390:133–160

Vogt BA (2005) Pain and emotion interactions in subregions of the cingulate gyrus. Nat Rev Neurosci 6:533–545

Vogt BA, Rosene DL, Pandya DN (1979) Thalamic and cortical afferents differentiate anterior from posterior cingulate cortex in the monkey. Science 204:205–207

Vogt BA, Pandya DN, Rosene DL (1987) Cingulate cortex of rhesus monkey I. Cytoarchitecture and thalamic afferents. J Comp Neurol 262:256–270

Vogt BA, Aston-Jones G, Vogt LJ (2008) Shared norepinephrinergic and cingulate circuits, nociceptive and allostatic interactions and cingulate contributions to functional pain and stress disorders. In: Vogt BA (ed) Cingulate neurobiology and disease, Chap. 22 (in press)

Westlund KN, Craig AD (1996) Association of spinal lamina I projections with brainstem catecholamine neurons in the monkey. Exp Brain Res 110:151–162

Willis WD Jr, Kenshalo DR, Leonard RB (1979) The cells of origin of the primate spinothalamic tract. J Comp Neurol 188:543–574

Woulfe JM, Flumerfelt BA, Hrycyshyn AW (1990) Efferent connections of the A1 noradrenergic cell group: a DBH immunohistochemical and PHA-L anterograde tracing study. Exp Neurol 109:308–322

Yasui Y, Itoh K, Takada M, Mitani A, Kaneko T, Mizuno N (1985) Direct cortical projections to the parabrachial nucleus in the cat. J Comp Neurol 234:77–86